Proc. Estonian Acad. Sci. Phys. Math., 1995, 44, 2/3, 317–326
https://doi.org/10.3176/phys.math.1995.2/3.21

RENORMALIZATION OF ELEMENTARY EXCITATIONS OF THE t-J MODEL WITH DOPING

Alexei SHERMAN[a] and Michael SCHREIBER[b]

[a] Eesti Teaduste Akadeemia Füüsika Instituut (Institute of Physics, Estonian Academy of Sciences), Riia 142, EE-2400 Tartu, Eesti (Estonia)

[b] Institut für Physik, Technische Universität Chemnitz-Zwickau (Technical University of Chemnitz-Zwickau), D-09107 Chemnitz, Deutschland (Germany)

Received 1 August 1994, accepted 17 April 1995

Abstract. Hole and magnon spectral functions of the 2D t-J model are self-consistently calculated from a set of Dyson's equations for the hole concentrations $x \lesssim 0.3$. For $J \ll t$, it is shown that near $x = 0.05$ the hole spectrum changes drastically, acquiring features of a weakly correlated spectrum. This change is accompanied by the entering of the chemical potential μ into a sharp maximum of the density of states. With x increasing the maximum moves together with μ up to $x \approx 0.15$ and then lags behind. This concentration is also distinctive in that the Fermi surface becomes a simply connected surface and the overdamped magnons which appear near $x = 0.02$ occupy the widest region in k space. Besides, a limiting frequency of usual magnons passes through a minimum here. Significant deviations from the normal Fermi liquid, which partly resemble the marginal Fermi liquid, are observed for $x \gtrsim 0.05$.

Key words: high-T_c superconductivity, t-J model.

The extended Hubbard model [1] and the related t-J model are widely accepted for the description of CuO_2 planes of cuprate perovskites. Keeping in mind a comparison with the experiment and the investigation of superconductivity, a consideration of these models for moderate hole concentrations is of special interest. In this paper such a consideration is carried out on the basis of the spin–wave approximation [2, 3]. It allows one to investigate the lattices which are large enough to avoid finite-size effects [4]. On the other hand, the approximation has been shown to be remarkably accurate in the description of the properties of both undoped and lightly doped crystals [5–7].

As has been shown previously [8, 9], for the parameters [10] which are adequate for La_2CuO_4, the extended Hubbard Hamiltonian can be transformed to the t-J Hamiltonian. In the spin–wave approximation the latter can be written in the form [2, 3, 7]

$$H = \sum_{\mathbf{k}\mathbf{k}'} (g_{\mathbf{k}\mathbf{k}'} h^{\dagger}_{\mathbf{k}} h_{\mathbf{k}-\mathbf{k}'} b_{\mathbf{k}'} + \text{H.c.}) + \sum_{\mathbf{k}} \omega^{0}_{\mathbf{k}} b^{\dagger}_{\mathbf{k}} b_{\mathbf{k}}, \qquad (1)$$

where $h_{\mathbf{k}}^{\dagger}$ is the fermion creation operator of a hole with the wave vector $\mathbf{k}$ in the classical Néel state $|\mathcal{N}\rangle$ which is the vacuum state for the boson spin–wave operator $b_{\mathbf{k}}$. With good accuracy these two operators can be considered as independent for the states of interest [3]. In Eq. (1), $\omega_{\mathbf{k}}^{0} = 2J\sqrt{1-\gamma_{\mathbf{k}}^{2}}$ is the unperturbed magnon frequency with the superexchange constant J and $\gamma_{\mathbf{k}} = [\cos(k_x a) + \cos(k_y a)]/2$, a is the intersite distance which is taken as the unit of length. The interaction constant $g_{\mathbf{k}\mathbf{k}'} = -4t(\gamma_{\mathbf{k}-\mathbf{k}'}u_{\mathbf{k}'} + \gamma_{\mathbf{k}}v_{\mathbf{k}'})/\sqrt{N}$ comprises the effective hopping constant t and the number of sites N, $u_{\mathbf{k}} = \cosh(\alpha_{\mathbf{k}})$, $v_{\mathbf{k}} = -\sinh(\alpha_{\mathbf{k}})$, $\alpha_{\mathbf{k}} = \ln[(1+\gamma_{\mathbf{k}})/(1-\gamma_{\mathbf{k}})]/4$. Terms of the static hole interaction and of the spin–bond softening near holes [7, 9] are omitted in Eq. (1) since their influence is small for the considered hole concentrations. This point will be discussed later in more detail.

For the considered low temperatures, the zero-temperature hole and magnon Green's functions, $G(\mathbf{k}, t-t') = -i\langle \mathcal{T} h_{\mathbf{k}}(t) h_{\mathbf{k}}^{\dagger}(t')\rangle$ and $D(\mathbf{k}, t-t') = -i\langle \mathcal{T} b_{\mathbf{k}}(t) b_{\mathbf{k}}^{\dagger}(t')\rangle$, can be used, where $\mathcal{T}$ is the time ordering operator. The related hole and magnon spectral functions, $A(\mathbf{k}\omega) = -\operatorname{Im} G(\mathbf{k}\omega)/\pi$ and $B(\mathbf{k}\omega) = -\operatorname{Im} D(\mathbf{k}\omega)/\pi$, are calculated from the following set of Dyson's equations [11]:

$$
\begin{aligned}
\operatorname{Im}\Sigma(\mathbf{k}\omega) &= \begin{cases} -\sum\limits_{\mathbf{k}'} g_{\mathbf{k}\mathbf{k}'}^{2} \int_{0}^{\omega-\mu} \dfrac{d\omega'}{\pi} \operatorname{Im} G(\mathbf{k}-\mathbf{k}', \omega-\omega') \operatorname{Im} D(\mathbf{k}'\omega'), \\ \qquad\qquad \text{for } \omega > \mu, \\ -\sum\limits_{\mathbf{k}'} g_{\mathbf{k}-\mathbf{k}',-\mathbf{k}'}^{2} \int_{0}^{\mu-\omega} \dfrac{d\omega'}{\pi} \operatorname{Im} G(\mathbf{k}-\mathbf{k}', \omega+\omega') \times \\ \qquad \times \operatorname{Im} D(\mathbf{k}'\omega'), \text{ for } \mu > \omega, \end{cases} \\
\operatorname{Re}\Sigma(\mathbf{k}\omega) &= \mathcal{P}\int_{-\infty}^{\infty} \frac{d\omega'}{\pi} \frac{\operatorname{sgn}(\omega'-\mu)\operatorname{Im}\Sigma(\mathbf{k}\omega')}{\omega'-\omega}, \\
\operatorname{Im}\Pi(\mathbf{k}\omega) &= \begin{cases} \sum\limits_{\mathbf{k}'} g_{\mathbf{k}'\mathbf{k}}^{2} \int_{\mu-\omega}^{\mu} \dfrac{d\omega'}{\pi} \operatorname{Im} G(\mathbf{k}', \omega+\omega') \operatorname{Im} G(\mathbf{k}'-\mathbf{k}, \omega'), \\ \qquad\qquad \text{for } \omega > 0, \\ \sum\limits_{\mathbf{k}'} g_{\mathbf{k}'\mathbf{k}}^{2} \int_{\mu}^{\mu-\omega} \dfrac{d\omega'}{\pi} \operatorname{Im} G(\mathbf{k}', \omega+\omega') \operatorname{Im} G(\mathbf{k}'-\mathbf{k}, \omega'), \\ \qquad\qquad \text{for } \omega < 0, \end{cases} \\
\operatorname{Re}\Pi(\mathbf{k}\omega) &= \mathcal{P}\int_{-\infty}^{\infty} \frac{d\omega'}{\pi} \frac{\operatorname{sgn}(\omega')\operatorname{Im}\Pi(\mathbf{k}\omega')}{\omega'-\omega},
\end{aligned}
\tag{2}
$$

where $\Sigma(\mathbf{k}\omega)$ and $\Pi(\mathbf{k}\omega)$ are the hole and the magnon self-energies, $G(\mathbf{k}\omega) = [\omega - \Sigma(\mathbf{k}\omega)]^{-1}$, $D(\mathbf{k}\omega) = [\omega - \omega_{\mathbf{k}}^{0} - \Pi(\mathbf{k}\omega)]^{-1}$, μ is the chemical potential of holes. On derivation of Eqs. (2) vertex corrections were neglected, which is usually referred to as the self-consistent Born

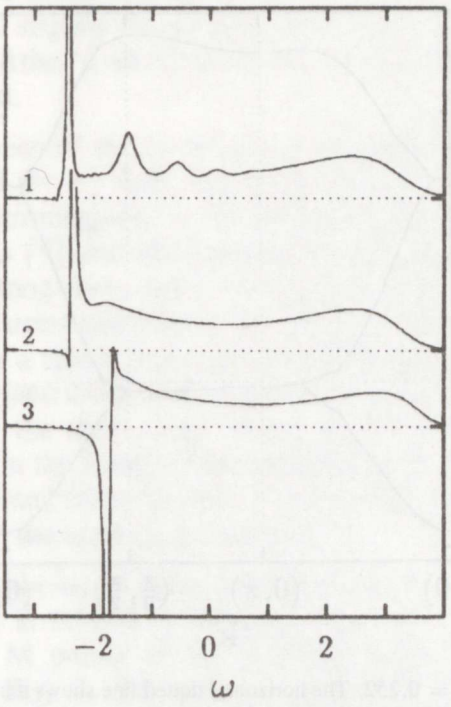

Fig. 1. The hole spectral function $A(\mathbf{k}\omega)$. Curves 1 to 3 correspond to $x = 0.005$, 0.058, and 0.252 ($\mu = -2.6$, -2.4, and -1.7, respectively); $\mathbf{k} = (0, \pi)$, $J = 0.2$, $\eta = 0.015$. The dotted lines indicate the zero levels of the spectral function, the scale is arbitrary.

approximation [12]. The smallness of these corrections for $x \ll 1$ was demonstrated in [11]. Since normal-state properties are considered, anomalous Green's functions are not included in Eqs. (2).

This set of equations was solved iteratively on a discrete mesh of k and ω points. A 20×20 lattice was used. On the basis of the estimated parameters [10] of La_2CuO_4 the effective superexchange constant $J = 0.2$ was selected (here and below all energy parameters are given in units of t). In this case the main part of $A(\mathbf{k}\omega)$ is in the frequency range from -5 to 4. This spectral function was computed on 400 equally spaced points in this range, while the magnon spectral function $B(\mathbf{k}\omega)$ was computed in the range from -0.4 to 0.8 (the limiting frequency of unperturbed magnons $2J = 0.4$). An artificial broadening $\eta = 0.015$ was introduced into Green's functions to make the iterative procedure stable.

A principal conclusion following from the results obtained is a sharp change of the character of the hole energy spectrum near $x = 0.05$ (the hole concentration is calculated from the chemical potential according to $x = \sum_{\mathbf{k}} \int_{-\infty}^{\mu} d\omega \, \mathrm{Im}\, G(\mathbf{k}, \omega)/\pi N$). Figure 1 demonstrates this statement for one of the wave vectors.

For $x \lesssim 0.05$ $A(\mathbf{k}\omega)$ is similar to the one obtained for a solitary hole [4] (the uppermost curve in Fig. 1). The spectra contain a series of maxima corresponding to quasiparticle states forming narrow energy bands with

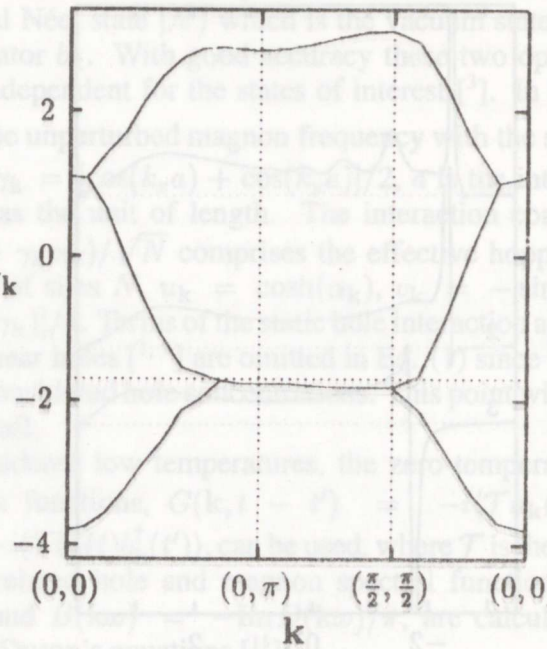

Fig. 2. Energy bands at $x = 0.252$. The horizontal dotted line shows the position of the chemical potential.

bandwidths of the order of J. When x approaches 0.05, the major part of these maxima disappears and for larger concentrations only two or three maxima, depending on $\mathbf{k}$ and μ, remain. On plotting the central frequencies of these maxima versus the wave vector, the energy structure shown in Fig. 2 is obtained. Excluding the uppermost curve, it can be seen that the remaining curves are similar in their shape to two energy bands of uncorrelated carriers with nearest neighbour hopping in a lattice with a doubled period. Naturally, in comparison with the bands spanning the energy range from -4 to 4, the bands in Fig. 2 are significantly distorted. In particular, instead of the zero-frequency portion of the uncorrelated bands, which is positioned along the boundary of the magnetic Brillouin zone, the obtained curves have a weakly dispersive portion which remains near the chemical potential, moving together with it, up to the largest considered concentration $x = 0.294$ ($\mu = -1.5$). However, in spite of these differences, as in the uncorrelated case, the bands are characterized by bandwidths of the order of t. Thus, in a comparatively narrow range of concentrations near $x = 0.05$ a transition takes place from heavy to much lighter carriers.

At the same time, for $x \gtrsim 0.05$ spectra retain some features of low-concentration spectra. Among them is the uppermost band in Fig. 2 which has a prototype in the latter spectra. The common portion of the two lower bands, which is positioned near μ, can simultaneously be considered as the second feature of the kind. This portion is formed by sharp maxima which

originate from the lowest maxima of low-concentration spectra. For the x which are only slightly larger than 0.05, this portion of the bands has extensions beyond the "weakly correlated" bands and hence retains features of a separate band.

This coexistence of the properties of weakly and strongly correlated systems observed for $x \gtrsim 0.05$, can be related to the establishment of the short-range antiferromagnetic ordering induced by doping. In accordance with the previous [11] and the present calculations this takes place near $x = 0.02$. In the long-range order, which exists at smaller x, any jump of a hole on a neighbouring site leads to the creation or destruction of a magnon (see Eq. (1)). As a result, there appears a spin polaron with a substantial magnon cloud around a hole and narrow bands. A deviation from this ideal ordering such as the short-range order reveals underlying wider energy bands contained in the Hamiltonian (recall that the hole transport term in Eq. (1) was obtained from the nearest neighbour hopping term of the t-J Hamiltonian with the hopping constant t).

In the used spin–wave description the destruction of the long-range order mentioned is related to the appearance of overdamped magnons near the Γ and M points of the Brillouin zone [11]. This behaviour is illustrated by Fig. 3. For a wave vector from the vicinity of the Γ point and a sufficiently large concentration the magnon spectral function contains a band whose central frequency is much smaller than its width (curves 2 to 4). Thus, the corresponding excitation has a nearly purely imaginary frequency. Such excitations do not appear in a periphery of the magnetic Brillouin zone. To appreciate the relation between the destruction of the long-range order and the overdamped magnons, let us note that their appearance means that the respective magnon occupation numbers become indefinite. This fact indicates that the spin–wave approximation in itself becomes inapplicable for certain ranges in the crystal. Their size and shape depend on the size and shape of the regions in the reciprocal space where overdamped magnons are located. For x which are only slightly above 0.02 the sizes of these regions around the Γ and M points are approximately equal to k_F, the Fermi momentum measured from the momentum of the ground state $(\pi/2, \pi/2)$ [11]. This means that the spin–wave approximation is applicable for the regions of a direct space with sizes smaller than $\xi \approx k_F^{-1}$ and inapplicable for larger regions. In turn, this means that there is no correlation between the alignment of spins over a distance larger than ξ. In this picture overdamped or relaxational magnons can be related to a stochastic relative movement of quantization axes in the regions of the size ξ. Thus, the appearance of such magnons at some critical concentration of holes means the destruction of the long-range antiferromagnetic order, presumed by the spin–wave approximation, and the emergence of a short-range order with the instantaneous spin correlation length $\xi \approx k_F^{-1} \approx a/\sqrt{x}$. This dependence of the in-plane correlation length on the concentration has earlier been observed for small x in $La_{2-x}Sr_xCuO_4$ [13, 14].

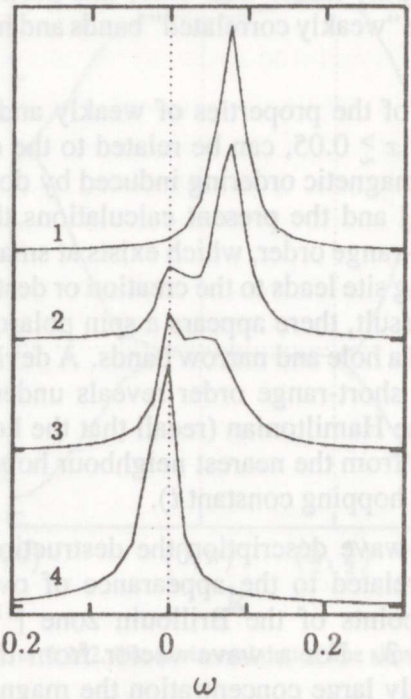

Fig. 3. The magnon spectral function $B(\mathbf{k}\omega)$. $\mathbf{k} = (0, \pi/10)$; curves 1 to 4 correspond to $x = 0.01$, 0.022, 0.045 ($\mu = -2.52, -2.47, -2.45$), and 0.252, respectively.

Since the system considered is a two-dimensional one, for which the long-range antiferromagnetic ordering is known [15] to be impossible for any nonzero temperature, the following additional remarks should be made. For the temperatures $T \ll J/k_B \approx 1000\,\mathrm{K}$ the correlation length determined by temperature fluctuations is exponentially large [16], $\xi' \sim \exp(J/k_B T)$, much larger than ξ. Thus, the appearance of overdamped magnons means a drastic decrease of the in-plane spin correlation length. Taking into account that due to a small value of the interplane exchange constant [13] large 2D regions of ordered spins play the crucial role in establishing the 3D long-range ordering [16], the critical concentration for the appearance of overdamped magnons can be related to the hole concentration destroying the 3D long-range ordering in a crystal. It is worth noting that the obtained value, $x \approx 0.02$, is really close to the one derived experimentally [13, 14, 17]. This point was discussed in more detail in [11].

For $x \lesssim 0.03$ the branch of overdamped magnons coexists with the usual magnon branch in the small regions of the Brillouin zone mentioned. This coexistence manifests itself in two well-resolved maxima in the spectral function (curve 2 in Fig. 3) . For larger concentrations these maxima coalesce gradually (curves 3 and 4) and the portion of the usual magnon branch disappears near the Γ and M points. With x increasing up to 0.15 the regions of the Brillouin zone occupied by overdamped magnons

continue to grow. Accordingly, the spin correlation length ξ continues to decrease. For $x > 0.15$ this growth is altered with a slow decrease with the respective weak increase of ξ. A similar behaviour of the spin correlation length, starting at somewhat smaller concentrations, has been observed in $La_{2-x}(Ba, Sr)_xCuO_4$ [14].

The obtained magnon spectral function demonstrates a significant softening of the usual magnon branch with the increase of x up to $x \approx 0.15$ where the limiting frequency of this branch is approximately three times smaller than $2J$. For larger concentrations the softening is altered by a growing rigidity. It should be noted, however, that the boundary concentration, $x \approx 0.15$, can be somewhat changed by holding the term of the spin–bond softening near a hole [7] in Hamiltonian (1). This term is local and for spatially uniform states its influence can be approximately taken into account by introducing the factor $(1 - x)$ into the second term in the right-hand side of Eq. (1). Since the obtained boundary concentration is small, only a minor correction to its value can be expected. However, for larger concentrations this process will lead to a new magnon softening with a growing damping and, finally, to a complete destruction of the magnon branch.

The concentration $x = 0.15$ is also distinctive in the circumstance that near it the Fermi surface becomes a simply connected surface. For this and smaller concentrations the Fermi surface has a considerable scope for nesting.

The hole density of states $\rho(\omega) = \mathrm{sgn}(\omega - \mu) \sum_{\mathbf{k}} \mathrm{Im}\, G(\mathbf{k}, \omega)/\pi$ is depicted in Fig. 4 for several values of x. This quantity has a pronounced maximum connected with the lowest spin polaron band in the case $x \lesssim 0.05$ and with states near the boundary of the magnetic Brillouin zone for larger concentrations. As noted above, this part of the energy surface originates from the band and therefore partly retains its large spectral intensity. On the other hand, this portion contains a van Hove singularity, the saddle point, which is analogous to that of uncorrelated bands. Thus, for $x \gtrsim 0.05$ the maximum is contributed from these two sources. From Fig. 4 it can be seen that starting from $x \approx 0.05$ the chemical potential falls on the maximum. Together with μ the maximum is shifted to higher frequencies. As a consequence, the chemical potential is kept in the maximum in a considerable range of concentrations, approximately up to $x = 0.15$. Near this concentration the density of states at μ reaches its peak. After this the maximum begins to lag behind the chemical potential.

This result is a clear argument in favour of the van Hove scenario for superconductivity (see [18] and references therein). However, it should be borne in mind that the maximum in the density of states is only partly connected with the van Hove singularity. The obtained characteristic concentrations, $x \approx 0.05$ and $x \approx 0.15$, in accordance with this scenario corresponding to a minimal concentration for superconductivity and to maximal T_c, are in reasonable agreement with experiment on $La_{2-x}Sr_xCuO_4$ [13, 14, 19]. The results of [19], obtained for this crystal,

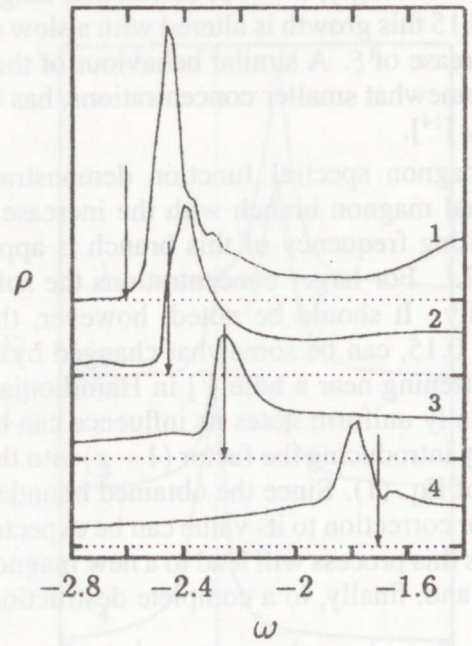

Fig. 4. The hole density of states. Curves 1 to 4 correspond to $x = 0.005$, 0.045, 0.11 ($\mu = -2.25$), and 0.252, respectively. The dotted lines indicate the zero levels. The arrows show the positions of the chemical potential.

apparently confirm the fact that the density of states at μ goes through a maximum simultaneously with T_c near $x = 0.16$.

In conclusion, let us discuss some general properties of the hole ensemble. For extremely small hole concentrations it can easily be seen from Eqs. (2) that near the Fermi level $\mathrm{Im}\,\Sigma \sim (\omega - \mu)^2$, the result which is inherent for a normal Fermi liquid [12]. Perceptible deviations from this behaviour start near $x = 0.05$. The dependence can approximately be described by the power law with an exponent which is a trifle over unity for $x \lesssim 0.15$ and slightly below it for larger concentrations. Thus, for $x \gtrsim 0.05$ holes cease to be a normal Fermi liquid. The proximity of the obtained dependence, $\mathrm{Im}\,\Sigma(\omega)$, to the linear one makes the hole ensemble similar to the marginal Fermi liquid [20]. However, there are two essential differences from the basic concept of [20]. Firstly, the slopes below and above the Fermi level are, in general, substantially different and, secondly, there is a strong dependence of the hole damping on $\mathbf{k}$.

In summary, hole and magnon spectral functions of the 2D t-J model were self-consistently calculated for the hole concentrations $x \lesssim 0.3$. It was shown that there exist four ranges of concentrations characterized by qualitatively different spectra. In the first range, $x \lesssim 0.02$, the spectra are similar to the ones obtained for a solitary hole having narrow bands of spin polarons. In the second range, $0.02 \lesssim x \lesssim 0.05$, a branch of overdamped magnons reveals itself in the magnon spectral function, indicating the

destruction of the long-range antiferromagnetic order. At $x \approx 0.05$, at the beginning of the third range, the hole spectrum changes drastically, acquiring the features of a weakly correlated spectrum. It is characterized by a considerably smaller effective mass of carriers and a sharp maximum of the density of states which falls on the chemical potential. This situation clearly promotes superconductivity. In this range pronounced deviations in the behaviour of the hole ensemble from a normal Fermi liquid are observed. Up to the upper concentration of this range, $x \approx 0.15$, the k-space region occupied by overdamped magnons grows, while the frequencies of usual magnons decrease considerably. At the beginning of the fourth range the Fermi surface becomes a simply connected surface. With x increasing the sharp maximum in the density of states begins to move away from the chemical potential, the region of overdamped magnons becomes narrower and usual magnon frequencies grow.

REFERENCES

1. Emery, V. J. Phys. Rev. Lett., 1987, **58**, 2794.
2. Schmitt-Rink, S., Varma, C. M., Ruckenstein, A. E. Phys. Rev. Lett., 1988, **60**, 2793; Kane, C. L., Lee, P. A., Read, N. Phys. Rev. B, 1989, **39**, 6880.
3. Sherman, A. V. Solid State Commun., 1990, **76**, 321; Physica C, 1990, **171**, 395.
4. Marsiglio, F., Ruckenstein, A. E., Schmitt-Rink, S., Varma, C. M. Phys. Rev. B, 1991, **43**, 10882.
5. Huse, D. A. Phys. Rev. B, 1988, **37**, 2380; Chakravarty, S., Halperin, B. I., Nelson, D. R. *ibid.*, 1989, **39**, 2344.
6. Sabczynski, J., Schreiber, M., Sherman, A. Phys. Rev. B, 1993, **48**, 543.
7. Sherman, A. V. Physica C, 1993, **211**, 329.
8. Zhang, F. C., Rice, T. M. Phys. Rev. B, 1988, **37**, 3759.
9. Sherman, A. V. Phys. Rev. B, 1993, **47**, 11521.
10. McMahan, A. K., Annett, J. F., Martin, R. M. Phys. Rev. B, 1990, **42**, 6268.
11. Sherman, A., Schreiber, M. Phys. Rev. B, 1993, **48**, 7492; 1994, **50**, 12887.
12. Abrikosov, A. A., Gor'kov, L. P., Dzyaloshinskii, I. E. Methods of Quantum Field Theory in Statistical Physics. Pergamon Press, New York, 1965.
13. Birgeneau, R. J., Shirane, G. – In: Ginsberg, D. M. (ed.). Physical Properties of High Temperature Superconductors. World Scientific, Singapore, 1989.
14. Aeppli, G., Hayden, S. M., Mook, H. A., Mason, T. E., Taylor, A. D., Clausen, K. N., Perring, T. G., Cheong, S.-W., Fisk, Z., Rytz, D. Physica B, 1993, **192**, 103.
15. Mermin, N. D., Wagner, H. Phys. Rev. Lett., 1966, **17**, 1133.
16. Capellmann, H., Lötfering, J., Schärpf, O. Z. Phys. B, 1992, **88**, 181.
17. Rossat-Mignod, J., Regnault, L. P., Bourges, P., Vettier, C., Burlet, P., Henry, J. Y. Physica B, 1993, **186–188**, 1.
18. Newns, D. M., Krishnamurthy, H. R, Pattnaik, P. C., Tsuei, C. C., Chi, C. C., Kane, C. L. Physica B, 1993, **186-188**, 801.
19. Loram, J. W., Mirza, K. A. – In: Kuzmany, H., Mehring, M., Fink, J. (eds.). Electronic Properties of High-T_c Superconductors and Related Compounds. Springer Series in Solid-State Sciences. Springer-Verlag, Berlin, 1990, **99**.
20. Varma, C. M., Littlewood, P. B., Schmitt-Rink, S., Abrahams, E., Ruckenstein, A. E. Phys. Rev. Lett., 1989, **63**, 1996.

ELEMENTAARERGASTUSTE ÜMBERNORMIMINE LEGEERIMISEGA t-J MUDELIS

Aleksei ŠERMAN, Michael SCHREIBER

Aukude kontsentratsiooni intervalli $x \leq 0,3$ jaoks on isekooskõlaliselt arvutatud vaskperovskiitide kahemõõtmelise t - J mudeli aukude ja magnonite spektraalsed funktsioonid. Juhu $J \ll t$ puhul on näidatud, et kontsentratsiooni $x = 0,05$ ümbruses muutub järsult aukude energeetiline spekter, omandades nõrgalt korreleeritud süsteemile iseloomulikke jooni. Sama kontsentratsiooni korral saavad märgatavaks aukude ansambli olulised erinevused Fermi vedelikust, meenutades osalt marginaalset Fermi vedelikku. Kontsentratsioonil $x \approx 0,05$ siseneb keemiline potentsiaal olekute tiheduse teravasse maksimumi. Olekute tihedus keemilisel potentsiaalil saavutab maksimumi, kui $x \approx 0,15$, ja kahaneb kiiresti $x > 0,25$ puhul. Fermi pind muutub ühelisidusaks $x \approx 0,15$ korral. Aukude spektri nimetatud muutused on seotud antiferromagnetilise kaugkorrastuse kadumise ja lähikorrastuse tekkega $x \approx 0,02$ korral. Ülesumbunud magnonite täiendava haru tekkimine nimetatud kontsentratsioonil on selle faasisiirde väljenduseks magnonite spektris. $x \approx 0,15$ korral on nende magnonite poolt hõivatud k-ruumi piirkond maksimaalne, harilike magnonite piirsagedus aga minimaalne.

ПЕРЕНОРМИРОВКА ЭЛЕМЕНТАРНЫХ ВОЗБУЖДЕНИЙ t–J-МОДЕЛИ С ДОПИРОВАНИЕМ

Алексей ШЕРМАН, Михаэль ШРАЙБЕР

Для интервала концентраций дырок $x \leq 0,3$ самосогласованно вычислены дырочные и магнонные спектральные функции двумерной t–J-модели купратных перовскитов. Для случая $J << t$ показано, что вблизи концентрации $x = 0,05$ энергетический спектр дырок резко меняется, приобретая черты спектра слабокоррелированной системы. При этой же концентрации становятся заметными существенные отличия ансамбля дырок от жидкости Ферми, отчасти напоминающие маргинальную жидкость Ферми. При $x \approx 0,05$ химический потенциал дырок входит в резкий максимум плотности состояний. Плотность состояний на химическом потенциале достигает максимума при $x \approx 0,15$ и быстро убывает для $x > 0,25$. Поверхность Ферми становится односвязной при $x \approx 0,15$. Указанные изменения дырочного спектра связаны с разрушением дальнего антиферромагнитного порядка и установлением ближнего при $x \approx 0,02$. Возникновение дополнительной ветви передемпфированных магнонов при указанной концентрации служит проявлением этого фазового перехода в магнонном спектре. При $x \approx 0,15$ область k-пространства, занимаемая этими магнонами, максимальна, а предельная частота обычных магнонов - минимальна.